Coordinating Cascaded Surge Protection Devices: High-Low versus Low-High

Jih-Sheng Lai
Power Electronics Application Center
Knoxville TN

François D. Martzloff
National Institute of Standards and Technology
Gaithersburg MD
f.martzloff@ieee.org

Reprinted, with permission, from *IEEE Transactions on Industry Applications IA-29*, July/August 1993
First presented as ICPSD 91-28 at the IEEE-IAS Annual Meeting, Dearborn, 1991

Significance:
Part 8 – Coordination of cascaded SPDs

For a “cascade” of two MOV-based SPDs, the combined numerical modeling and the laboratory measurements cross-validate to provide information on the relationship of impinging waveform and amplitude, distance between the two SPDs, and relative values of the SPD limiting voltage.

Results show that separate selection of the service entrance SPD and point-of-use SPD can produce an ineffective coordination, with the point-of-use SPD “protecting” the service entrance SPD and in so doing, take on the dissipation of a disproportionate part of the impinging surge energy.

This situation make the case for giving careful attention to the selection of device parameters, such as providing the two devices from an authoritative source from which a well-engineered approach should be expected.

Coordinating Cascaded Surge Protection Devices: High-Low versus Low-High

Jih-Sheng Lai and François D. Martzloff, *Fellow, IEEE*

Abstract— **Cascading surge protection devices located at the service entrance of a building and near the sensitive equipment is intended to ensure that each device shares the surge stress in an optimum manner to achieve reliable protection of equipment against surges impinging from the utility supply. However, depending on the relative clamping voltages of the two devices, their separation distance, and the waveform of the impinging surges, the coordination may or may not be effective. The paper provides computations with experimental verification of the energy deposited in the devices for a matrix of combinations of these three parameters. Results show coordination to be effective for some combinations and ineffective for some others, which is a finding that should reconcile contradictory conclusions reported by different authors making different assumptions. From these results, improved coordination can be developed by application standards writers and system designers.**

I. Introduction

RECENT PROGRESS in the availability of surge-protective devices, combined with increased awareness of the need to protect sensitive equipment against surge voltages, has prompted the application of a multistep cascade protection scheme. In the multistep cascade scheme, a high-energy surge protective device would be installed at the service entrance of a building for the purpose of diverting the major part of the surge energy. Then, surge-protective devices with lower energy-handling capability and lower clamping voltage than that of the service entrance would be installed downstream and complete the job of protecting sensitive equipment at the point of entry of the line cord. To make the distinction between these two devices, we will call the service entrance "arrester" and the downstream device "suppressor," somewhat in keeping with U.S. usage of the transient voltage surge suppressor (TVSS) for devices used on the load side of the mains disconnect. Such a scheme is described as "coordinated" if, indeed, the device with high-energy handling capability receives the largest part of the total energy involved in the surge event.

Paper ICPSD 91-28, approved by the Power Systems Protection Committee of the IEEE Industry Applications Society for presentation at the 1991 Industry Applications Society Annual Meeting, Dearborn, MI, September 28–October 4. This work was supported by the Electric Power Research Institute, Power Electronics and Control Program, Customer Systems Division. Contributions from U.S. Government personnel are not protected by U. S. Copyright. Manuscript released for publication September 11, 1992.

J. -S. Lai was with the Power Electronics Applications Center, Knoxville, TN 37932. He is now with the Engineering Technology Division, Oak Ridge National Laboratory, Oak Ridge, TN 37831-7280.

F. D. Martzloff is with the National Institute of Standards and Technology, Gaithersburg, MD 20899.

IEEE Log Number 9210072.

This scenario was based on the technology of secondary surge arresters prevailing in the 1970's and early 1980's as well as on the consensus concerning the waveform and current levels of representative lightning surges impinging on a building service entrance. This consensus has gradually evolved toward recognition that the surge environment may include waveforms of longer duration than the classical 8/20 μs current surge. ANSI/IEEE C62.41–1991 [1] provides a description of the surge environment. With the emergence of new types of arresters for service entrance duty and the recognition of waveforms with greater duration than the classic 8/20 μs impulse, a new situation arises that may invalidate the expectations of the cascade coordination scenario.

Service entrance arresters were generally based on the combination of a gap with a nonlinear varistor element, which was the classic surge arrester design before the advent of metal-oxide varistors that made gapless arresters possible. With a gap-plus-varistor element, the service entrance arrester could easily be designed for a 175-V maximum continuous operating voltage (MCOV) in a 120-V (rms) system. The downstream suppressors were selected with a low level, driven by the perception that sensitive equipment requires a low protective level [2]. The scheme can work if there is a series impedance (mostly inductance) between the arrester and the suppressor because the inductive drop in the series impedance, added to the clamping voltage of the suppressor, becomes high enough to spark over the arrester gap. Thereafter, the lower discharge voltage of the arrester (made possible by the gap) ensures that the major part of the surge energy is diverted by the arrester, relieving the suppressor from heavy duty [3].

Now, if the arrester is of gapless type, its MCOV will determine its clamping level. Some utilities wish to ensure survival of the arrester under the condition of a lost neutral, that is, twice the normal voltage for a single-phase, three-wire service connection. The "high-low" combination has been proposed, where the arrester clamping voltage is higher than that of the suppressor [4]. During the ascending portion of a relatively steep surge such as the 8/20 μs, the inductive drop may still be sufficient to develop enough voltage across the terminals of the arrester and force it to absorb much of the impinging energy. However, during the tail of the surge, the situation is reversed; the inductive drop is now negative, and thus, the suppressor with lower voltage (not the arrester) will divert the current. For the new waveforms proposed in C62.41–1991 [1], this situation occurs for the 10/1000 μs where the tail contains most of the energy, and the relief provided by the arrester may not last past

0093-9994/93$03.00 © 1993 IEEE

TABLE I
CURVE FITTING RESULTS FOR CIRCUIT MODELING OF THREE MOV'S

MOV number	k	α	λ	ζ	V_0(V)
V130LA20A	4.0×10^{-74}	30	0.051	8×10^{-6}	320
V150LA20A	3.9×10^{-89}	35	0.053	4×10^{-6}	370
V250LA40A	5.7×10^{-110}	40	0.04	4×10^{-6}	570

the front part of the surge. For the low-frequency (5 kHz or less) capacitor-switching ring waves, the inductive drop will be much smaller than that occurring with the 8-μs rise time so that the additional voltage may be negligible, leaving the suppressor in charge from the beginning of the event. An alternate means has been proposed (Low-High) where the arrester clamping voltage is lower than that of the suppressor [5], [6]. Thus, a disagreement has emerged among the recommendations for coordinated cascade schemes: the 1970–1980 perception and [4], suggesting a "High-Low" and the new "Low-High" suggestion of [5] and [6].

This paper reports the results of modeling the situation created by the emergence of gapless arresters and longer waveforms with the necessary experimental validation. These results cover a range of parameters to define the limits of a valid cascade coordination and serve as input to the surge protective device application guides now under development by providing a reconciliation of the apparent disagreement, which is actually rooted in different premises on the coordination parameters.

II. MOV CIRCUIT MODELING

The current-voltage (I-V) characteristic of a metal oxide varistor (MOV) has long been represented by an exponential equation, i.e., $I = kV^{\alpha}$ [7]. This equation is only applicable in a certain voltage (current) range in which the I-V characteristic presents a linear relationship in a log-log plot. When the voltage exceeds this "linear region," the current increment rate starts dropping. A modified I-V characteristic is proposed here as expressed in (1).

$$I = kV^{\alpha} e^{-(V-V_0)(\lambda-\zeta(V-V_0))}. \quad (1)$$

The parameters in (1) can be obtained from a minimum-error-norm curve fitting technique [8] using a manufacturer's data book [7] or experimental results. The parameters k and α can be obtained from fitting the data in the linear log-log region. The exponential term is added to cover the voltages that are higher than a threshold voltage V_o and can be obtained from fitting the I-V characteristics in the higher current (voltage) region. Using (1), the MOV circuit model can be simply represented by a voltage-dependent current source.

Model parameters in (1) can be obtained from the manufacturer's data book and verified by experiments. The parameter is typically a function of the MOV voltage rating. The threshold voltage V_0 and coefficients λ and ζ are functions of the voltage rating and the size. Table I lists curve fitting results for the

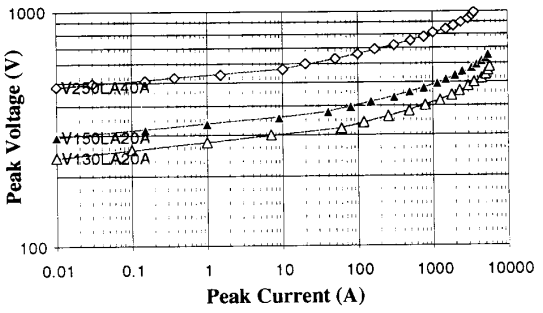

Fig. 1. MOV characteristics obtained from modeling results.

TABLE II
PARAMETERS FOR NOMINAL I-V CHARACTERISTICS OF THREE MOV'S

MOV number	k	α	λ	ζ	V_o(V)
V130LA20A	9.4×10^{-66}	27	0.046	0.8×10^{-6}	285
V150LA20A	4.8×10^{-79}	31.5	0.053	1.6×10^{-6}	340
V250LA40A	1.7×10^{-97}	36	0.044	1.6×10^{-6}	520

equivalent circuit parameters of three MOV's for units of voltage and current in volts and amperes.

The MOV number[1] actually reflects the device voltage rating and the size. For V130LA20A, the continuous operating voltage rating is 130 V(rms). The other two devices are 150 and 250 V(rms), respectively. All three devices have a 20-mm diameter. Fig. 1 shows fitted curves for the three devices.

In Fig. 1, the marked dots were the data directly obtained from the manufacturer's data book, whereas the three solid lines were calculated from (1) using the parameters listed in Table I.

It should be noted that each individual MOV may have slightly different I-V characteristics even with the same model number. In Fig. 1, the data show the maximum clamping voltage levels, which are 10% higher than the nominal voltage level. A typical off-the-shelf device has a tolerance within $\pm 10\%$ of the nominal voltage level, which means a lowest-level device could have an I-V characteristic that is 20% lower than the data book characteristics. In fact, the two closely rated cascading devices (130 and 150 V) could, in some extreme cases, become inverted in the sequence ("Low-High" becoming in reality "High-Low") as 130 × 1.1 = 143 and 150 × 0.9 = 135. Furthermore, the results show that for the 250-150 combination, the difference is so large that a low 250 (225 V) combined with a high 150 (165 V) would not make an appreciable difference in energy sharing. Thus, the simulation computations were performed for all three devices at their nominal values. From the maximum voltage tolerance parameters listed in Table I, the parameters for the nominal (zero tolerance) I-V characteristics were derived, as listed in Table II.

[1]Certain commercial products are identified in this paper in order to adequately specify the experimental procedure. Such identification does not imply recommendation or endorsement by the Power Electronics Applications Center or the National Institute of Standards and Technology, nor does it imply that the products are necessarily the best for the purpose.

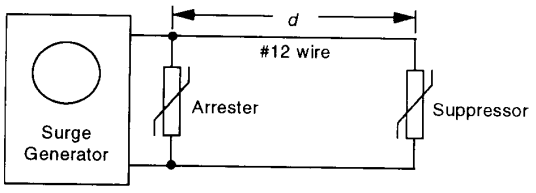

Fig. 2. Two-stage cascade surge protection system.

TABLE III
NINE POSSIBLE CASCADE COMBINATIONS FOR THREE DEVICES

Arrester	Suppressor
250 V	250 V
	150 V
	130 V
150 V	250 V
	150 V
	130 V
130 V	250 V
	150 V
	130 V

III. SIMULATION OF CASCADED SURGE PROTECTION DEVICES IN A LOW-VOLTAGE SYSTEM

In a two-stage cascade surge protection system, the arrester is placed near the surge source (the service entrance for premises wiring), and the suppressor is placed near the load. Fig. 2 shows a typical two-stage cascade surge protection system. The arrester and the varistor are separated by a distance d, which depends on the specific installation. In the following simulation study, four different d values are considered. They are 5, 10, 20, and 40 m. The #12 wire is a typical size for the premises wiring and is used for the following simulation and experiment study. Based on an impedance-meter measurement, the resistance of #12 wire is 0.00104 Ω/m, and the inductance is 1 μH/m (per two parallel wires). For high-frequency waves (the 1.2/50 – 8/20μs Combination Wave and the 0.5μs – 100 kHz Ring Wave), the inductive drop is the more dominant [9]. The complete simulation consists of a surge source, two voltage-dependent current sources, and a line impedance between the two current sources [10].

For the three selected device voltage levels, there is a total of nine possible cascade combinations as shown in Table III. Three standard waves from [1] were chosen to cover different frequency responses. These are 1.2/50 – 8/20μs Combination Wave, 0.5 – 100 kHz Ring Wave, and 10/1000μs impulse wave. For the sake of brevity, these three waveforms will be called "Combo Wave," "Ring Wave," and "Long Wave." For four distances, three voltage waves, and nine cascade combinations, a total of 108 cases were studied in the simulation: about 200 hours of machine time on a 25-MHz personal computer.

A. Simulation Results with the Combination Wave

Because of the back filter effect, a waveform generator might not couple a true standard wave to the test circuit. Fig. 3 shows an oscillation of the standard 8/20μs current wave. Curve A is the standard 8/20μs current, and curve B is the actual coupled wave with a small negative swing. For the standard 8/20μs wave, the current is always positive, and the clamping voltage is always positive. When applying curve B as the surge source, the negative current portion will cause a negative clamping voltage. This has been observed in the experiments. In order to reflect the experimental results, the following simulation will use curve B as the combo wave source.

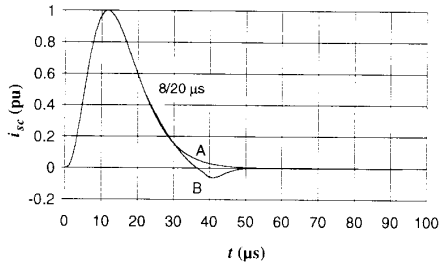

Fig. 3. Standard 8/20 μs short-circuit wave and a possible negative swing caused by the filtering circuit.

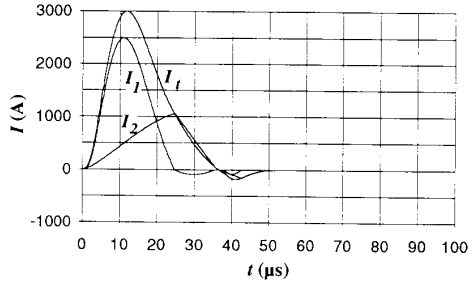

Fig. 4. Simulated Combo Wave current responses for the 250–130V cascaded devices that are 10-m apart.

Consider a 250–130 V cascade of two devices that are 10 m apart. The simulation results of the currents flowing in the two devices are shown in Fig. 4, where I_t is the total current injected into the cascade by the surge source of the model, I_1 is the arrester current, and I_2 is the suppressor current. Fig. 5 shows device clamping voltages with V_1 and V_2 representing arrester and suppressor voltage, respectively. Fig. 6 shows instantaneous powers with P_1 and P_2 representing arrester and suppressor power, respectively. By integrating the instantaneous power, the energy deposition values in the arrester and the suppressor were calculated as 29.7 and 8.6 J, respectively.

Before proceeding with further simulations, the simulation results were verified by an experiment. With the experimental setup of Fig. 2 and 250 and 130 V rated devices in cascade, the experimental results for the arrester and suppressor are shown in Fig. 7. Because the surge generator generates nonstandard waveforms, the waveforms obtained from the experiment are not exactly the same as the simulated waveforms. However, the power distribution between the two devices shows good agreement between simulation and experiment. For the same

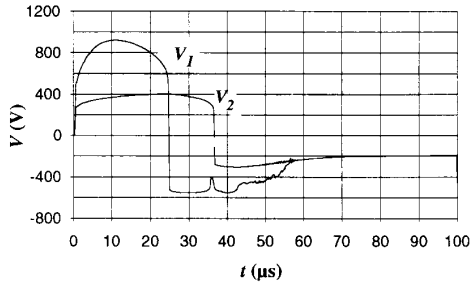

Fig. 5. Simulated Combo Wave voltage responses for the 250–130 V cascaded devices that are 10-m apart.

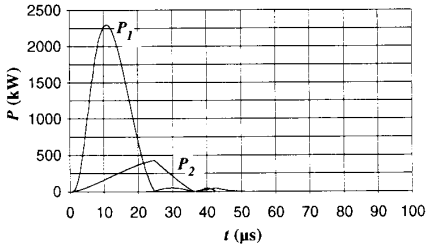

Fig. 6. Simulated Combo Wave power responses for the 250–130V cascaded devices that are 10-m apart.

250–130, 10-m cascaded case but slightly higher peak surge current (3.3 kA instead of 3 kA in simulation), the experimental result shows 33.8 and 11.1 J energy depositions in the arrester and the suppressor, respectively. Prorating the simulation results from Fig. 6 to 3.3 kA would yield 32.7 and 9.5 J, respectively, which is a reasonable agreement.

Table IV lists Combo Wave simulation results of the energy deposition in the arrester (A) and suppressor (S) for all the combinations of different High-Low and Low-High cascade conditions. For the High-Low condition, the energy deposition in the suppressor increases when the distance decreases. This result explains how the High-Low configuration can achieve a good coordination under the Combo Wave, provided that there is sufficient distance between the two devices, as stated in [3].

Consider the High-Low configuration with a 250-V device as the arrester. When the distance between two devices is reduced, the energy deposition tends to increase in the suppressor and decrease in the arrester. This decrease occurs because the line inductance does not provide enough voltage drop ($L\ \mathrm{d}i/\mathrm{d}t$), and the low clamping voltage of the suppressor reduces the voltage across the arrester and thus reduces the energy deposition level. The total energy deposition in the two devices also varies with the distance for the High-Low configuration. In Table IV, the total energy deposition for the 250–250 combination is near constant at 103 J for different distances. However, for the 250–150 and 250–130 combinations, the total energy deposition decreases when the distance is reduced because the suppressor tends to lower the voltage across the arrester.

For Low-High configurations such as the 150–250 and 130–250 cases, the high-voltage suppressor receives almost zero energy. The use of the suppressor is near redundant

TABLE IV
ENERGY DEPOSITION IN THE CASCADED DEVICES WITH A 3-kA COMBO WAVE AS THE SURGE SOURCE

Clamping voltage of device (V)		Distance separating devices and energy deposited in each device (J)							
		5 m		10 m		20 m		40 m	
A	S	A	S	A	S	A	S	A	S
250	250	75.9	27.3	83.5	19.9	89.5	14.4	91.7	9.69
	150	22.2	12.0	29.9	8.52	35.9	5.40	39.80	3.30
	130	21.3	11.9	29.7	8.6	35.3	5.2	40.1	3.3
150	250	24.3	0.005	24.3	0.006	24.3	0.007	24.3	0.008
	150	21.2	4.65	23.1	3.06	24.4	1.93	25.5	0.88
	130	19.84	5.16	22.16	3.05	24.05	1.86	25.02	1.08
130	250	22.9	0.003	22.9	0.003	22.9	0.004	22.9	0.004
	150	20.2	1.72	20.8	1.18	21.30	0.76	21.1	0.44
	130	18.6	2.92	19.4	1.71	20.3	1.03	20.9	0.70

in this case, except for its application to mitigate internally generated surges. With closely rated devices (130–150), the 150-V voltage suppressor also receives much less energy than the 130-V arrester.

B. Simulation Results with the 0.5 μs–100 kHz Ring Wave

The energy deposition in the surge protection devices under the Ring Wave surge is considerably less than that of the Combo Wave because of lower current. However, the high-frequency Ring Wave shows similar characteristics to the Combo Wave under the High-Low cascade condition; a voltage drop between the two devices can be established by the line inductance, provided that there is sufficient distance between the two devices. Figs. 8 and 9 show simulation results of current and voltage for the cascaded arrester and suppressor under the High-Low condition. I_1 and V_1 represent the 250-V arrester current and voltage, whereas I_2 and V_2 represent the 130-V suppressor current and voltage, respectively, for a 400-A peak surge current.

Fig. 10 shows the instantaneous power dissipated in the two cascaded devices. P_1 and P_2 represent the 250-V arrester power and 130-V suppressor power, respectively.

Table V lists the simulated energy deposition in the cascaded devices for different High-Low and Low-High combinations. The energy is the integration of the instantaneous power over the total 20-μs simulation period. Unlike the Combo Wave, the Ring Wave tail still contains a small amount of power, and the total amount of the energy deposition is affected by the integration interval. From Fig. 10, it is apparent that the power contribution to the total (past 20 μs) is becoming negligible.

Similar to the Combo Wave, the High-Low configuration shows good coordination as the high-voltage arrester absorbs higher energy under the high-frequency Ring Wave surge, and the Low-High configuration shows almost zero energy deposition in the high-voltage suppressors.

C. Simulation Results with the 10/1000 μs Long Wave

Compared with the Combo Wave, the Long Wave has a slower and longer drooping tail that contains most of the surge energy. During the long tail period, the inductive voltage drop between the arrester and the suppressor is low due to low $L\mathrm{d}i/\mathrm{d}t$, and the voltage across the arrester is reduced by the

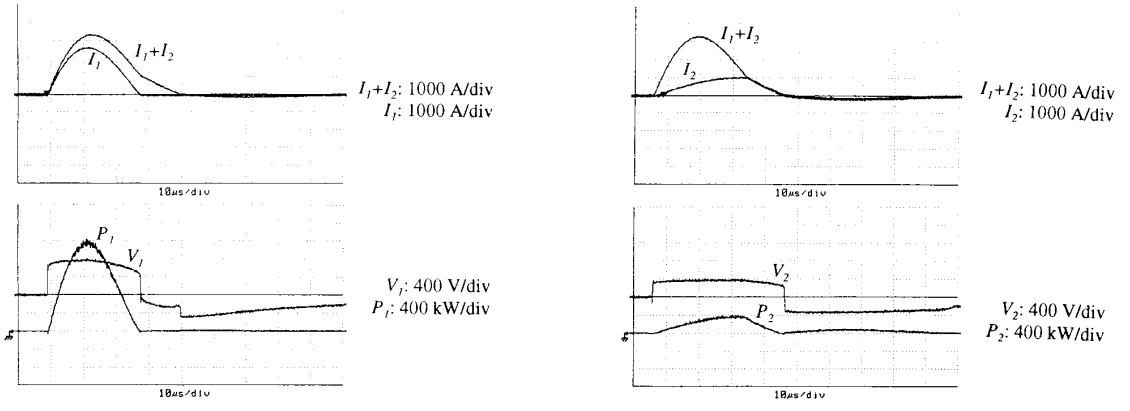

Fig. 7. Experimental results for the 250–130 V cascade with devices that are 10-m apart, with the Combination Wave: (a) Arrester; (b) suppresor.

TABLE V
ENERGY DEPOSITION IN THE CASCADED DEVICES WITH A 400-A PEAK RING WAVE AS THE SURGE SOURCE

Clamping voltage of device (V)		Distance separating devices and energy deposited in each device (J)							
		5 m		10 m		20 m		40 m	
A	S	A	S	A	S	A	S	A	S
	250	1.287	0.398	1.405	0.291	1.512	0.158	1.593	0.114
250	150	0.996	0.625	1.301	0.317	1.536	0.127	1.613	0.094
	130	0.938	0.501	1.213	0.312	1.425	0.183	1.624	0.083
	250	1.21	0.002	1.21	0.003	1.21	0.003	1.21	0.004
150	150	1.05	0.15	1.11	0.097	1.15	0.059	1.17	0.035
	130	0.945	0.218	1.06	0.127	1.13	0.07	1.17	0.04
	250	0.99	.0006	0.99	.0005	0.99	.0004	0.99	.0003
130	150	0.97	0.020	0.97	0.019	0.97	0.019	0.97	0.017
	130	0.90	0.123	0.96	0.078	0.99	0.049	1.010	0.278

suppressor even with long distance between the two devices. This makes the High-Low configuration not coordinated as the high-voltage arrester will not absorb any impinging energy, but the suppressor does. Figs. 11, 12, and 13 show the simulated Long Wave current, voltage, and power, respectively, for the arrester and the suppressor under a High-Low (250–130) configuration for a 200-A peak surge current.

The high-voltage arrester clamps the voltage during the impulse rising period and draws a small amount of the current pulse I_1, which is almost invisible in the computer-generated plot of Fig. 11. The power absorbed by the arrester P_1 is also a small pulse that appears at the rising period as shown in Fig. 13. The low-voltage suppressor absorbs all the impinging energy in this High-Low configuration, defeating the intended coordination.

Table VI lists the simulated energy deposition in the cascaded devices for different High-Low and Low-High combinations as well as for different distances.

It can be seen from Table VI that the low-voltage device always absorbs higher energy than the high-voltage device because the voltage across the high-voltage device is clamped to the same level as that of the low-voltage device, and the energy is diverted to the low-energy device. Unlike the Combo Wave and the high-frequency Ring Wave, the coordination for

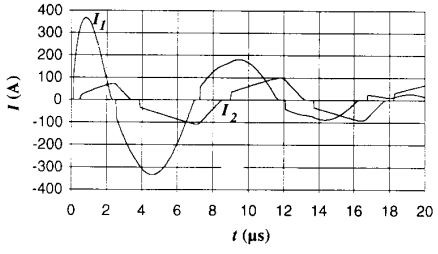

Fig. 8. Simulated Ring Wave current responses for the 250–130 V cascaded devices that are 10-m apart.

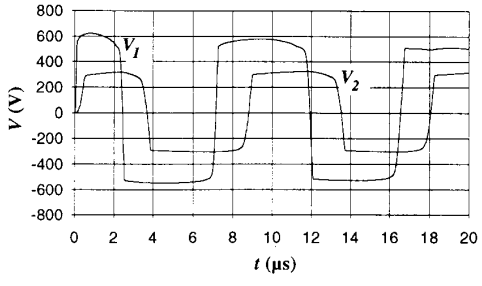

Fig. 9. Simulated Ring Wave voltage responses for the 250–130 V cascaded devices that are 10-m apart.

the slow Long Wave can only be achieved by Low-High or equally rated devices (250-250, 150-150, and 130-130). Note that with two devices of equal nominal value, it is possible that the relative tolerance might, in fact, produce a High-Low situation, which would not achieve good coordination; for instance, a 150-130 combination resulting from tolerance shifts imposes a 70-J duty to the suppressor in the case of 5-m separation.

IV. EXPERIMENTAL RESULTS

In order to verify the validity of the simulation, a series of experiments has been conducted using the three waves for different High-Low and Low-High combinations, especially

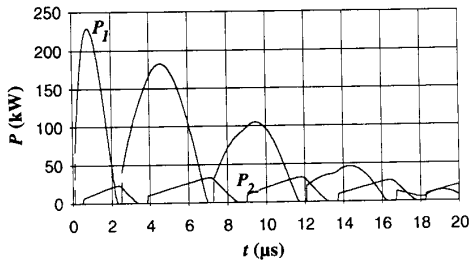

Fig. 10. Simulated Ring Wave instantaneous power for the 250–130 V cascaded devices 10-m that are apart.

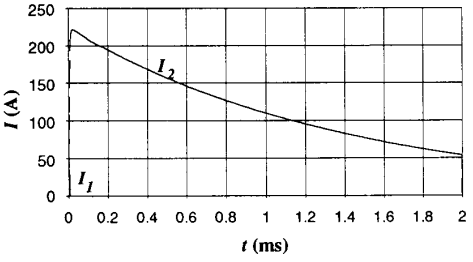

Fig. 11. Simulated Long Wave current responses for the 250–130 V cascaded devices that are 10-m apart.

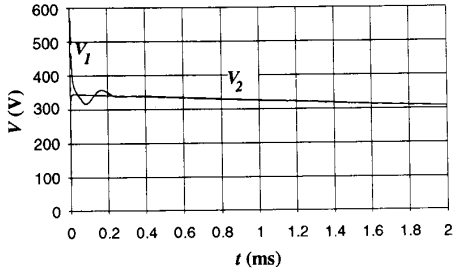

Fig. 12. Simulated Long Wave voltage responses for the 250–130 V cascaded devices that are 10-m apart.

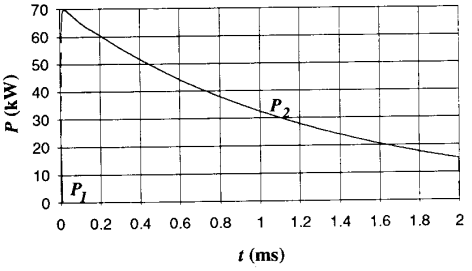

Fig. 13. Simulated Long Wave power responses for the 250–130 V cascaded devices that are 10-m apart.

TABLE VI
ENERGY DEPOSITION IN THE CASCADED DEVICES WITH A 220-A PEAK LONG WAVE SURGE SOURCE

Clamping voltage of device (V)		Distance separating devices and energy deposited in each device (J)							
		5 m		10 m		20 m		40 m	
A	S	A	S	A	S	A	S	A	S
250	250	73.63	72.76	74.10	72.31	75.06	71.38	76.28	70.13
	150	0.031	92.15	0.028	92.03	0.69	91.70	1.77	91.00
	130	0.011	79.23	0.125	79.16	0.518	78.94	1.424	78.42
150	250	92.17	0.001	92.17	0.002	92.17	0.002	92.17	0.003
	150	44.03	42.79	44.69	42.15	45.96	40.91	47.32	39.12
	130	7.92	70.67	8.86	69.76	10.72	67.97	14.28	64.58
130	250	79.20	0.001	79.20	0.001	79.20	0.001	79.20	0.001
	150	66.98	11.12	71.72	6.82	71.87	6.67	72.21	6.36
	130	38.03	36.74	38.70	36.09	39.98	34.84	42.28	32.62

TABLE VII
EXPERIMENTAL RESULTS USING DIFFERENT WAVEFORMS FOR 250–130 V CASCADED DEVICES THAT ARE 10-M APART

Applied Wave	Arrester			Suppressor		
	V_{pk} (V)	I_{pk} (A)	W (J)	V_{pk} (V)	I_{pk} (A)	W (J)
Combo 3 kA pk	790	2600	33.8	400	1000	11.1
Ring 430 A pk	720	340	0.6	350	100	0.2
Long 220 A pk	450	6	0.05	320	220	64.4*

for the Long Wave, which has not been used for cascaded coordination studies in the literature. Table VII lists experimental results (from Figs. 7, 14, and 15) using the three waveforms for 250–130 V cascaded devices that are 10-m apart. Note that peak currents do not occur simultaneously. A * sign shows that the low-voltage suppressor absorbs almost all the energy under the 10/1000 μs Long Wave. The experimental results, in general, agree with the simulation results, especially for the Combo Wave, which has well matched surge sources and a limited surge period (the tail does not extend over the integration period). For the Ring Wave and the long wave, the total integration period and the surge source are not matched between simulation and experiment, and thus, the numbers in Table VII have higher deviation from the simulation results. However, the proportion between the arrester and the suppressor energies agrees well between simulation and experiment, which explains that the simulation can be effectively used for the coordination analysis.

The experimental verification of the Combo Wave for the simulation can be seen from Fig. 7. For the Ring Wave and the Long Wave, experimental current, voltage, and power waves are shown in Figs. 14, 15, and 16, respectively. The Ring Wave coupled from the surge generator is distorted and is attenuated much faster than the standard Ring Wave. The measurement of the coupled Long Wave shows a saturation on the small CT (5000 A peak and 65 A rms rated). However, the current flowing through the surge protection devices were measured by a large CT (20 000 A peak and 325 A rated) and were not saturated.

The experimental Long Wave response for a Low-High configuration is shown in Fig. 16, where I_1 and I_2 are the currents flowing in the 130-V arrester and the 150-V suppressor, respectively. This figure shows an example of good coordination by Low-High, where most of the surge energy is absorbed by the low-voltage arrester. The arrester voltage V_1 is almost the same as the suppressor voltage V_2 with a slight difference at the beginning of the surge.

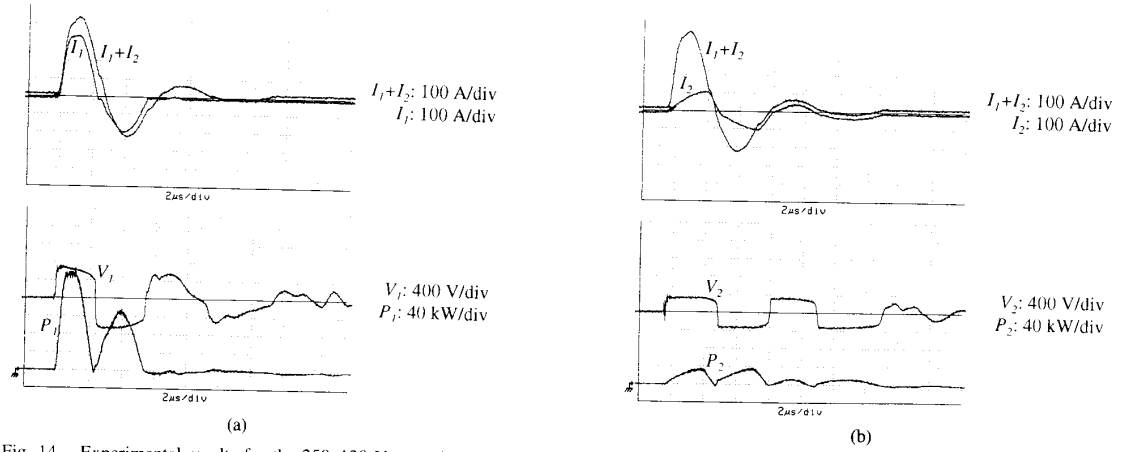

Fig. 14. Experimental results for the 250–130 V cascade, with devices that are 10-m apart, with the Ring Wave: (a) Arrester; (b) suppresor.

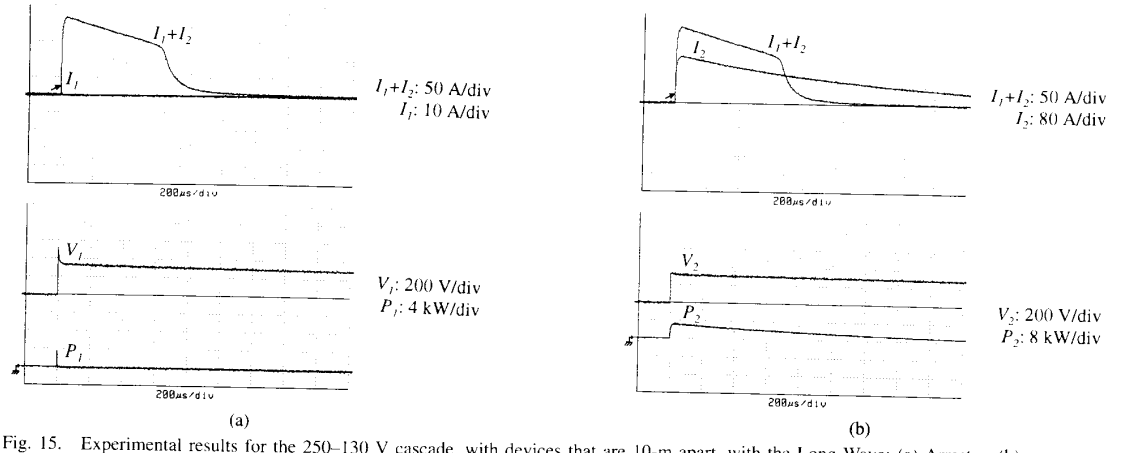

Fig. 15. Experimental results for the 250–130 V cascade, with devices that are 10-m apart, with the Long Wave: (a) Arrester; (b) suppresor.

V. Discussion

The concept of coordination of surge-protective devices is based on the selection of a first device with high energy-handling capability that is to be located at the service entrance and is expected to divert most of the surge current at that point. The second device, which is installed within the premises, can then have a lower energy-handling capability.

The benefit from this coordinated approach is to allow a single device at the service entrance to perform the high-energy duty, whereas several smaller devices within the premises can perform local suppression. This arrangement avoids the flow of large surge currents in the branch circuits of the installation, which is a situation known to produce undesirable side effects [11].

On the other hand, the situation where millions of small suppressors have been installed within equipment, or as plug-in devices, exists with only sporadic and anecdotal reports of problems. Thus, it is evidently possible to obtain protection with suppressors alone, whereas a coordinated scheme would provide additional benefits and eliminate side effects.

Some utilities wish to provide a service-entrance arrester thta is capable of withstanding the 240-V overvoltage that can occur on the 120-V branches when the neutral is lost.

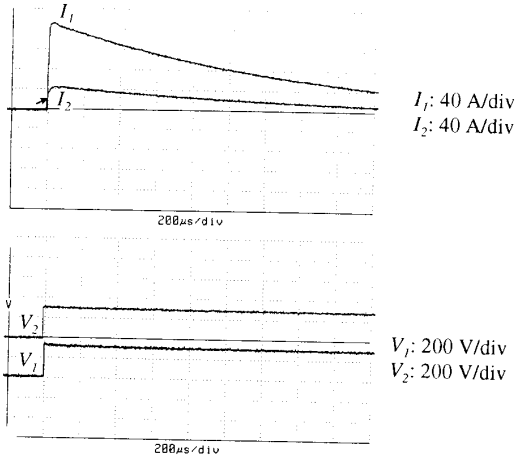

Fig. 16. Experimental results for the 130–150 V cascade, with devices that are 10-m apart, with the Long Wave.

This desire will force the coordination scheme into a High-Low situation because of the uncontrolled installation of low clamping voltage suppressors by the occupant of the premises. The results of the simulation and experimental measurements

show that the objective of coordination could still be achieved with a 250–130 combination, as long as some distance is provided between the two devices and as long as Long Waves are not occurring with high peak values. This proviso provides an incentive for obtaining better statistics on the occurrence of Long Waves. ANSI/IEEE C62.41-1991 [4] recommends considering these Long Waves as an additional and not a standard waveform. Thus, the determination of a successful coordination depends, for the moment, on the perception of what the prevailing high-energy waveforms can be for specific environments.

VI. Conclusions

1. Coordination of cascaded devices can be achieved under various combinations of parameters, but some combinations will result in having a suppressor with low energy-handling capability called on to divert the largest part of the surge energy. This uncoordinated situation can create adverse side effects when high current surges occur.
2. Significant parameters in achieving successful coordination involve three factors over which the occupant of the premises has no control: the relative clamping voltages of the two devices, their separation distance, and the prevailing waveforms for impinging surges. This uncontrolled situation presents a challenge and obligation for standards-writing groups to address the problem and develop consensus on a tradeoff of advantages and disadvantages of High-Low versus Low-High.
3. Coordinated schemes can be proposed by utilities to their customers, including a service entrance arrester and one or more plug-in devices to be installed for the dedicated protection of sensitive appliances. However, even such an engineered, coordinated arrangement could be defeated by the addition of a suppressor with a very low clamping voltage, which is not an insignificant likelihood in view of the present competition for lower clamping voltages.

VII. Update on Coordination Efforts

Since the presentation of the paper in the Fall of 1991, considerable discussion of the coordination issue has taken place at the international level involving five technical committees of the IEC. As of late 1992, an effort is underway within the IEC to develop an application document that will address the issues discussed in this paper and present recommendations tailored to the specific neutral-grounding practice of the various member countries. Contact the authors for further updates on progress concerning the technical aspects of device coordination issues as well as updates on the intercommittee coordination and liaison.

Acknowledgment

The authors wish to thank W. P. Malcolm of EPRI for his continued support. Thanks are also due to A. M. Maher and R. A. Veira of PEPCO and T. S. Key of PEAC for their encouragement in this project.

References

[1] ANSI/IEEE C62.41-1991, *IEEE Recommended Practice on Surge Voltages in Low-Voltage ac Power Circuits.*
[2] F. D. Martzloff and T. F. Leedy, "Selecting varistor clamping voltage: Lower is not better!" in *Proc. 1989 EMC Symp.* (Zürich).
[3] F. D. Martzloff, "Coordination of surge protectors in low-voltage ac power circuits," *IEEE Trans. Power App. Syst.*, vol. 99, pp. 129–133, Jan./Feb. 1980.
[4] M. F. Stringfellow and B. T. Stonely, "Coordination of surge suppressors in low-voltage ac power circuits," in *Proc. Open Forum Surge Protection Application*, NISTIR 4657, June 1991.
[5] R. B. Standler, "Coordination of surge arresters and suppressors for use on low-voltage mains," in *Proc. 1991 EMC Symp.* (Zürich).
[6] IEC 64/WG3 138A, "Explanation of interfaces for overvoltage categories," *Supplement to Appendix B of Rep. 664*, Nov. 1990.
[7] *Transient Voltage Suppression Devices*, Harris Corp., 1991.
[8] D. G. Luenberger, *Linear and Nonlinear Programming.* Reading, MA: Addison-Wesley, 1984.
[9] F. D. Martzloff, "On the propagation of old and new surges," in *Proc. Open Forum Surge Protection Application*, NISTIR 4657, June 1991.
[10] J. S. Lai, "Performance criteria for cascading surge-protective devices," in *Proc. Open Forum Surge Protection Application*, NISTIR 4657, June 1991.
[11] F. D. Martzloff, "Coupling, propagation, and side effects of surges in an industrial building wiring system," *IEEE Trans. Industry Applications*, vol. 26, no. 2, pp. 193–203, Mar./Apr. 1990.

Jih-Sheng (Jason) Lai is a native of Taiwan. He received the M.S. and Ph.D. degrees in electrical engineering from the University of Tennessee, Knoxville, in 1985 and 1989, respectively.

From 1980 to 1983, he was the Electrical Engineering Department Chairman of Ming-Chi Institute of Technology, Taipei, Taiwan, where he initiated a power electronic program and received a grant from the school and the National Science Council to study abroad. In 1989, he joined the EPRI Power Electronics Applications Center. He is currently the Power Electronics Lead Scientist at the Engineering Technology Division of the Oak Ridge National Laboratory. His main research interests are power electronics modeling and simulation, circuit design, and microcomputer applications. In the surge protection area, he developed varistor models and simulated cascaded surge protection circuits to understand more about fundamental concepts.

Dr. Lai has two patents in high-frequency power conversions for adjustable-speed drives and more than 25 articles published in the fields of control systems, power systems, and power electronics.

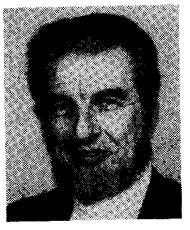

François D. Martzloff (F'83) is a native of France. After undergraduate studies there, he received the M.S.E.E. degree from Georgia Institute of Technology, Atlanta, in 1952 and the M.S.I.A. degree from Union College, Schenectady, NY, in 1972.

After 32 years in the private sector (Southern States Equipment from 1953–1956 and General Electric form 1956–1985), he joined the National Bureau of Standards, which is now the National Institute of Standards and Technology, Gaithersburg, MD. His early professional experience included the design of high-voltage fuses and bushings. He changed to semiconductor technology, but his high-voltage experience led him to the study of transients, which he has steadily pursued for the last 30 years. He has contributed a number of papers and led the development of several standards on surge characterization and surge testing.

Mr. Martzloff has been granted 13 patents, mostly on surge protection. In the IEEE, he serves as Chair of the Working Group on Surge Characterization. In the IEC, he is serving as Convenor of two working groups and chairs Subcommittee 77B (High-Frequency Phenomena) of TC77 on Electromagnetic Compatibility.